

# Hot-rolled Textures in 5083 Aluminum Alloy

Yuan Xiaokun, Cui Li

Beijing University of Technology, Beijing 100124, China

**Abstract:** The hot-rolled textures in a 5083 aluminum alloy were measured by electron backscattered diffraction (EBSD) technique. The results show that rolling texture components are uneven at different locations, and the grain boundary planes are textured. Grain boundary planes tend to the  $\{111\}$  orientation at the center of the specimen, and their amount is 50% higher than that of the random distribution case; grain boundary planes on the surface of the specimen tend to the  $\{110\}$  and  $\{112\}$  orientations, and their amount is 28% higher than that of the random distribution case. Moreover, anisotropic distribution of grain boundary planes appears at both low and high angle boundaries.

**Key words:** aluminum alloy; grain boundaries; hot rolled texture; electron backscattered diffraction; five parameter analysis

The low density, high strength, good formability and corrosion resistance make Al-Mg alloys particularly attractive in automobile, marine and aircraft applications. Hot rolling is one of the commonest thermomechanical treatments for processing aluminum within above applications, and recent researches prove that the hot-rolled textures have significant effect on the final anisotropy of the material performances<sup>[1]</sup>. Therefore, understanding textural developments in the hot rolling process is very important.

Grain boundary dependent properties are strongly determined by the crystallographic nature of the grain boundaries<sup>[2]</sup>. To quantitatively describe the type and frequency of grain boundaries, the concept of “grain boundary character distribution (GBCD)” was introduced<sup>[3]</sup>. Recently, “grain boundary engineering (GBE)” technique was developed to enhance the material’s performance by increasing the frequency of structurally ordered coincidence site lattice (CSL) boundaries with  $\Sigma \leq 29$ <sup>[3]</sup>. Electron backscattered diffraction (EBSD) technique has a superiority in statistically characterizing the distribution of boundary interfaces and therefore has become an effective tool for GBCD measurement. A recent development of EBSD technique is the stereological approach, named “five-parameter analysis (FPA)” method that comprehensively describes the grain boundary plane distribution (GBPD) within a polycrystalline structure through three Eulerian an-

gles to describe the lattice misorientation across the boundary plane and two spherical angles to describe the grain boundary plane orientation<sup>[4]</sup>. In addition, the validity of FPA method has been widely reported for a variety of materials<sup>[5]</sup>.

Each CSL boundary type corresponds to its habit planes with special geometries. Hence, GBPD characterizing is essential in the study of hot-rolled textures. However, only limited GBPD information can be found in previous works about aluminum alloys<sup>[6,7]</sup>. The present work gives a more comprehensive measurement about the hot-rolled textures in a typical Al-Mg alloy by FPA method, thus providing useful information for establishing the correlation between GBCDs and the performance of aluminum alloys.

## 1 Experiment

The selected 5083 Al-Mg alloy specimen was prepared by a semi-continuous casting method, with nominal composition of 4.20 wt% Mg, 0.73 wt% Mn, 0.11 wt% Zr, additional 0.46 wt% Er, and the balance Al. The ingot was homogenized at 470 °C for 20 h in an air-circulating oven, and then cut and milled. The ingot was then hot-rolled to a total reduction of 75% in thickness with a starting temperature of 450 °C and an ending temperature around 300 °C. The final thickness of the hot-rolled plate was 30 mm.

Two portions of the specimen were removed and mechani-

Received date: September 03, 2018

Foundation item: National Natural Science Foundation of China (51471007, 51475006)

Corresponding author: Yuan Xiaokun, Ph. D., Senior Experimentalist, College of Materials Science and Engineering, Beijing University of Technology, Beijing 100124, P. R. China, Tel: 0086-10-67396260, E-mail: bjutfive@163.com

Copyright © 2019, Northwest Institute for Nonferrous Metal Research. Published by Science Press. All rights reserved.

cally polished from cross sections perpendicular to the rolling plane (namely RD-TD plane): sample 1 (similarly hereinafter) was removed from the center of the specimen, and sample 2 (similarly hereinafter) was removed from the surface of the specimen. The EBSD measurements were performed using an Oxford Nordlys detector incorporated in a Zeiss Supra 55 scanning electron microscope. To ensure the accuracy of the measurements, the data were collected with a step size of 0.1  $\mu\text{m}$ , and then underwent a cleanup procedure to correct spurious points due to incorrect indexing. Because of the larger grain size, approximately 6000 grains for each sample were measured. Note that misorientation averaged data for FPA analysis in this work should be accurate with 2000 line segments for a face-centered cubic (fcc) system (this is not the case in Ref.[4], in which 50 000 line segments are needed for a complete FPA analysis, without averaging all misorientations). Hence, the collected data are sufficient for determining the GBPDs presented here.

The microtexture statistics were derived from TSL OIM<sup>TM</sup> Analysis 5.3 software. The observations needed for the FPA analysis are line segments extracted from the orientation maps and associated with the crystal orientations. The GBPDs were calculated using the stereological programs developed by Carnegie Mellon University, as described in Ref.[4]. Using the FPA method, the grain boundary distribution  $\lambda(\Delta g, n)$ , is defined as the relative areas of grain boundaries with a misorientation  $\Delta g$ , and boundary plane normal  $n$ , in units of multiples of a random distribution (MRD). Here, we only present  $\lambda(n)$ , which averages over all misorientations and gives the distribution of grain boundary planes in the crystal reference frame.

## 2 Results and Discussion

The microstructures of the selected partitions of the two samples are illustrated by the inverse pole figure (IPF) maps in Fig.1. In the figure, the grain color specifies the orientation according to the color indicated in the orientation legend. The images illustrate that grains on the surface suffer larger deformation and have a thinner shape than those at the center of hot rolled plate. To analyze the hot-rolled textures of the two samples, crystal orientation maps showing the volume fractions of the ideal rolling components are presented in Fig.2. In the figure, the grain color specifies textures according to the color indicated in the texture component legend. The images illustrate that the most prevalent textures are different in the two samples: the most prevalent textures in sample 1 are  $(231)\langle 3\bar{4}6 \rangle$  S3 and  $(110)\langle 1\bar{1}2 \rangle$  brass textures, accounting for 23.1 vol% and 17.5 vol%, respectively; however, the most prevalent textures in sample 2 are  $(241)\langle 1\bar{1}2 \rangle$  S1 and  $(4411)\langle 111\bar{1}8 \rangle$  Taylor textures, accounting for 12.4 vol% and 6.7 vol%, respectively. For further analysis, orientation distribution functions (ODFs) of the two samples are plotted into a reduced Euler space, as illustrated in Fig.3. In the figure, contours in units of MRD represent the distribution densities of the referred textures. It can

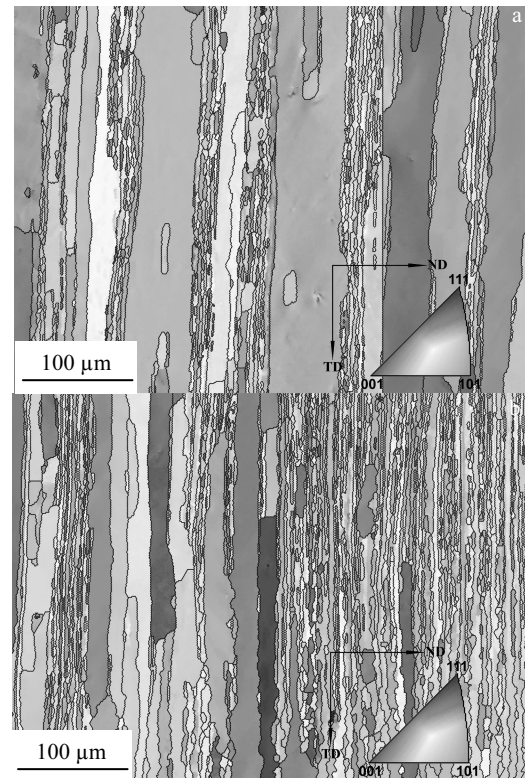


Fig.1 Inverse pole figure (IPF) maps of the selected portions of the two samples with orientations determined by the standard color coding scheme for cubic system: (a) sample 1 and (b) sample 2

be observed that the occurring locations of the major and secondary peaks for each sample are different, and such phenomenon can also illustrate that the prevalent grain orientation textures are different in the two samples.

Although Fig.2 and Fig.3 can illustrate grain orientation textures arised during the hot rolling, they cannot describe the textures of grain boundary planes. As a preparation for GBPD analysis, the distribution of misorientation angles between the aluminum alloy grains was calculated and the result is illustrated in Fig.4. The black line represents the misorientation distribution for an ideal random microstructure, and blue and red lines show the misorientation distributions of the grain boundaries in sample 1 and 2, respectively. It can be seen that the experimental distributions are clearly not random. Low angle boundaries (LABs) with misorientation angles lower than  $15^\circ$  are remarkably above the random, and high angle boundaries (HABs) with misorientation angles larger than  $15^\circ$  are beneath the random.

For these two samples, the GBPDs of  $\lambda(n)$ , which show the relative areas of grain boundary planes, are plotted in the crystal reference frame in Fig.5. In these distributions, values greater than one MRD indicate that the total area associated with a specific type of plane is larger than that expected in a random dis-

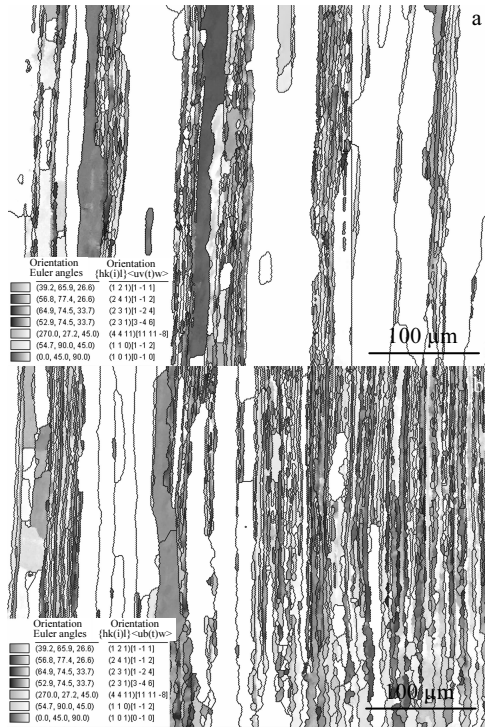


Fig.2 Crystal orientation maps showing the volume fractions of the ideal rolling components without considering the orthotropic variants: (a) sample 1 and (b) sample 2

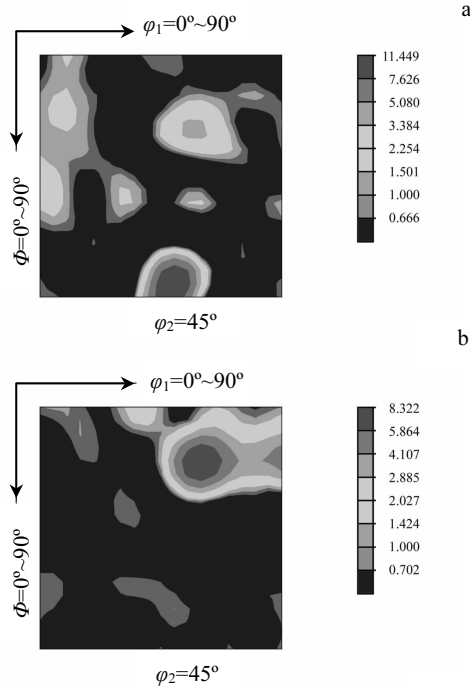


Fig.3 Orientation distribution function (ODF) maps of the two samples plotted in a reduced Euler space with units of the contours in MRD: (a) sample 1 and (b) sample 2

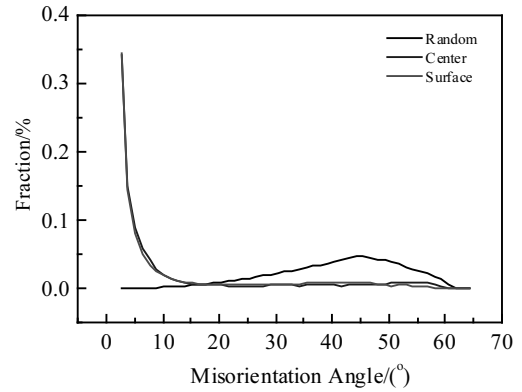


Fig.4 Grain boundary fraction and a random object as a function of misorientation angle

tribution, and values less than one MRD are associated with specific planes whose total areas are less than that expected in a random distribution. Note that for both samples, the GBPDs of entire grain boundaries are plotted at the first place, as presented in Fig.5a and Fig.5b. Then, according to Fig.4, the grain boundaries in both samples are sorted into LAB subsets and HAB subsets. Consequently, GBPDs of the LAB subsets are presented in Fig.5c and Fig.5d, and GBPDs of the HAB subsets are presented in Fig.5e and Fig.5f.

According to Fig.5a and Fig.5b, for entire grain boundaries in sample 1, the most frequently observed grain boundary plane orientation is  $\{111\}$  with a relative area 50% higher than that of the random distribution case; for sample 2, the maxima of the distribution are at  $\{110\}$  and  $\{112\}$  positions, and the relative area is 28% higher than that of the random distribution case, and it is also noted that the  $\{100\}$  orientations are the minimal positions for both samples. To explain the difference in the entire GBPDs, one can imagine that when materials undergo normal grain growth (not the case here), the grain boundary planes are generally inversely correlated to the grain boundary energy<sup>[5]</sup>. In aluminum alloys, the  $(111)$  surface has the lowest energy,  $(110)$  has the highest, and  $(100)$  is intermediate, while the total anisotropy is within 15%<sup>[8]</sup>, and boundaries based on  $\{111\}$  planes in fcc metals exhibit unusually low energies<sup>[9]</sup>. Measurements of the GBPD for commercially pure Al are consistent with this idea and show a maximum at the  $\{111\}$  orientation<sup>[10]</sup>. One can also imagine that in the hot rolling process, the surface of the slab typically experienced a higher deformation strain than the center, and grains on the surface hence have overall higher stored energies for recrystallization than at the center. Moreover, according to Fig.5c and Fig.5e for sample 1, the  $\{111\}$  planes keep as the most preferred boundary planes in both LAB and HAB subsets, but the frequency of occurrence varies from 1.92 MRD in Fig.5c to 1.5 MRD in Fig.5e, illustrating that  $\{111\}$  planes are more preferred in LABs than in HABs. According to Fig.5d and Fig.5f for sample 2, when

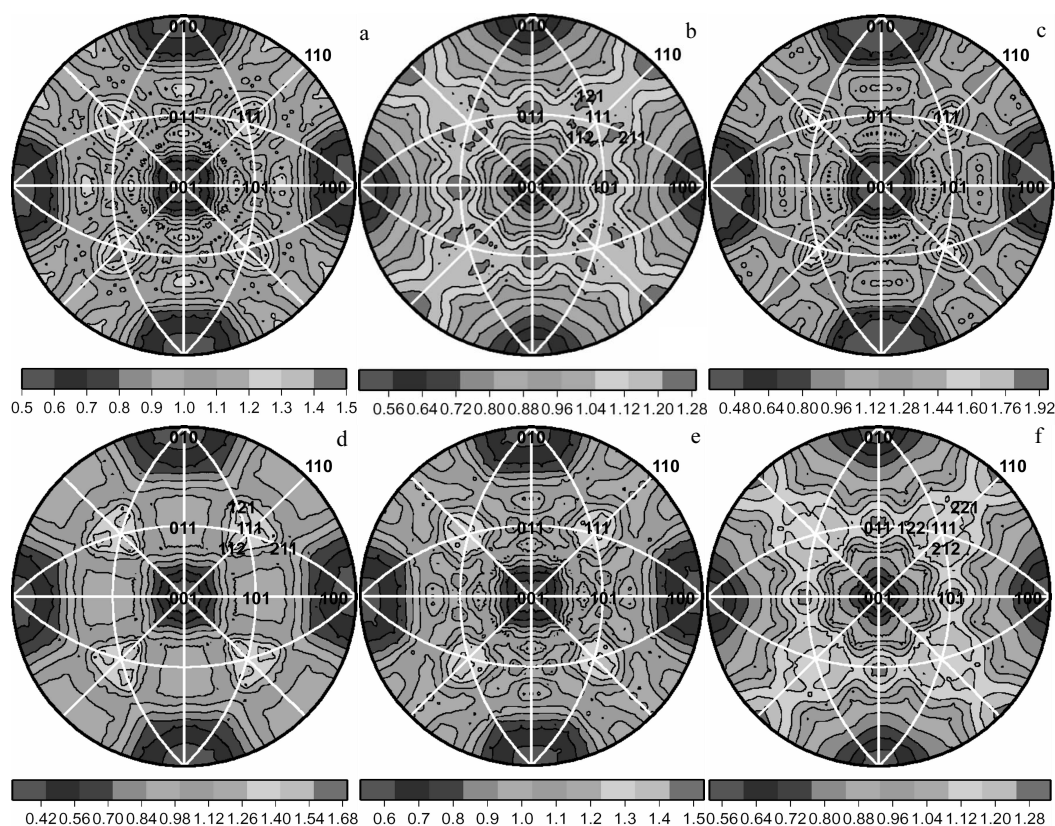


Fig.5 Misorientation averaged distribution of boundary planes for entire grain boundaries in sample 1 (a) and sample 2 (b); GBPDs of boundaries with misorientation angles lower than  $15^\circ$  in sample 1 (c) and sample 2 (d); GBPDs of boundaries with misorientation angles higher than  $15^\circ$  in sample 1 (e) and sample 2 (f) (stereographic projections are plotted along  $[001]$  direction, with units of the contours in MRD)

misorientation angles are lower than  $15^\circ$ , maxima are reached at  $\{112\}$  planes with a 1.68 MRD value, and for misorientation angles above  $15^\circ$ , a strong peak for  $\{110\}$  planes with a 1.28 MRD value and a smaller peak for  $\{122\}$  planes with a 1.20 MRD value can be observed. Note that the observed  $\{112\}$  planes deviate about  $20^\circ$  from  $\{111\}$  planes, and the observed  $\{122\}$  planes deviate about  $16^\circ$  from  $\{111\}$  planes; these boundary planes possibly represent the substructure created by the hot deformation. The above results demonstrate that different low index crystallographic planes are preferred at different locations within the ingot, and different planes are favored at different misorientation angles.

Except the disparity in deformation ratio at the center and surface positions in the hot-rolled aluminum alloys, the spatial diversity of temperature at these local positions should also be taken into account. For the grains at the center position (sample 1 in this work), the temperature gradient is relatively small due to the slow cooling process, so the local structure, with the orientation texture of boundary planes as the major proxy, is more prone to be adjusted to the  $\{111\}$  planes that have low-thermodynamical energies. Meantime, the grains at the

surface position (sample 2 in this work) are in the relatively large distortion state, so in this sense, most boundaries undergo the dislocation rearrangement, or just finish the dislocation rearrangement process; that is to say, the dislocation wall positions, containing  $\{110\}$  perfect dislocations or  $\{112\}$  imperfect dislocations in the fcc symmetries, have no time to adjust to the  $\{111\}$  planes. Such thermodynamical interpretation gives a more in-depth explanation about the GBPD results in Fig.5. In the upcoming work, heat-treatment will be loaded to the hot-rolled specimen so the evolution of GBPDs will be observed in more detail.

There are some indications that the retention of a high percentage of low energy boundaries offers an important approach for performance improvement through GBE. Taking corrosion resistance as an example, in most cases, the corrosion resistance increases if higher fraction of CSL boundaries with low  $\Sigma$  values can be obtained, and among these CSL boundaries, the  $\Sigma 3$  boundary containing  $(111)/(111)$  habit plane pairs (namely  $60^\circ/[111]$ ) is the most corrosion-resistant one (mostly developed during recrystallization but not the case of current work), and moreover, it is suggested that coherent twin  $\Sigma 3$  boundaries

have even higher corrosion resistance<sup>[11]</sup>. From the obviously observed GBPD results by the FPA method, it can be seen that compared to those on the surface of the specimen, grain boundary planes at the center of the specimen obviously favor the {111} orientation, which is possibly a necessary condition for a higher concentration of  $\Sigma 3$  boundaries. Therefore, it can be speculated that the center position has a higher corrosion resistance than the surface position of the selected specimen in this work, and hence, inducing the (111) planes as well as the concentration of  $\Sigma 3$  boundaries on the surface during recrystallization are reasonable approaches for improving the entire corrosion resistance of the hot-rolled specimen. From this point, the GBPD measurement presents a promising opportunity to establish the correlation between textures of grain boundary planes and the performance of aluminum alloys.

### 3 Conclusions

1) The hot-rolled texture in a 5083 aluminum alloy is measured, and the grain orientation textures and the preferential distribution of grain boundary planes are observed.

2) Grains situated at the slab center favor {111} orientations, and that situated at the slab surface prefer {110} and {112} orientations.

3) The preference for specific low index planes is different between low angle and high angle boundaries.

### References

- 1 Wells M A, Lloyd D J, Samarasekera I V et al. *Metallurgical and Materials Transactions B*[J], 1998, 29(3): 621
- 2 Randle V, Rohrer G S, Miller H M et al. *Acta Materialia*[J], 2008, 56(10): 2363
- 3 Watanabe T. *Journal of Materials Science*[J], 2011, 46(12): 4095
- 4 Saylor D M, Dasher B S, Adams B L et al. *Metallurgical and Materials Transactions A*[J], 2004, 35(7): 1981
- 5 Rohrer G S. *Journal of the American Ceramic Society*[J], 2011, 94(3): 633
- 6 Duan X, Sheppard T. *Modeling and Simulation in Materials Science and Engineering* [J], 2002, 10(4): 363
- 7 Uan J Y, Cheng H F. *Materials Transactions*[J], 2007, 48(2): 178
- 8 Nelson R S, Mazey D J, Barnes R S. *Theoretical Experimental and Applied Physics*[J], 1965, 11(109): 91
- 9 Wolf D. *Journal of Materials Research*[J], 1990, 5(8): 1708
- 10 Saylor D M, Dasher B S, Rollett A D et al. *Acta Materialia*[J], 2004, 52(12): 3649
- 11 Shimada M, Kokawa H, Wang Z J et al. *Acta Materialia*[J], 2002, 50(9): 2331

## 5083 铝合金中的晶界面热轧织构

原效坤, 崔 丽

(北京工业大学, 北京 100124)

**摘 要:** 通过电子背散射衍射(EBSD)技术, 测定了一种 5083 铝合金中的热轧织构。结果表明: 在结构中的不同位置, 织构组分呈现非均匀发展的特点, 特别地, 晶界面亦呈现取向织构。在样品的中心位置, 晶界面趋向于{111}取向, 且其数量高出随机晶界 50%; 同时, 在样品的边缘位置, 晶界面趋向于{110}与{112}取向, 且其数量高出随机晶界 28%。小角和大角晶界中均呈现这种晶界面的各向异性分布。

**关键词:** 铝合金; 晶界面; 热轧织构; 电子背散射衍射; 五参数法

作者简介: 原效坤, 男, 1974 年生, 博士, 高级实验师, 北京工业大学材料科学与工程学院, 北京 100124, 电话: 010-67396260, E-mail: bjutfive@163.com